顶强子谱学及势模型适用性的讨论

报告人：罗肆强

兰州大学

2026年03月28日

第五届强子与重味物理理论与实验联合研讨会

Si-Qiang Luo, Qi Huang, and Xiang Liu, arXiv:2508.17646 [hep-ph]

报告提纲

1. 研究背景
2. 模型方法
3. 数值结果
4. 总结

研究背景

实验

- 发现大量轻味介子
- 发现大量轻味重子
- 发现大量激发态强子（轻味、重味）
- 发现大量奇特强子态候选态

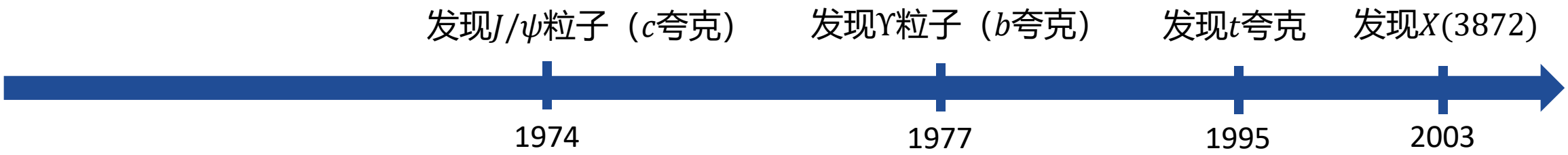

理论

- 对强子谱进行**定性**或**半定量**研究
- 建立早期的夸克模型（Gell-Mann、Zweig）
- 成功地预言了Ω粒子
- 发展了Cornell、Isgur-Karl、Godrey-Isgur、Capstick-Isgur模型
- 实现了对强子谱的**定量**计算
- 处理更复杂的谱学问题（反常谱学、紧致多夸克态、强子分子态、混杂态、胶球等）

✓ 传统的轻强子谱学

✓ 传统的粲强子、底强子谱学

✓ 反常谱学、奇特强子谱学

？ **顶强子谱学**

M. Gell-Mann, Phys. Lett. 8, 214–215 (1964).
G. Zweig, Version 1, 1964, 10.17181/CERN-TH-401.
G. Zweig, Version 2, 1964, 10.17181/CERN-TH-412.
V. E. Barnes et al., Phys. Rev. Lett. 12, 204–206 (1964).
(E598 Collaboration), Phys. Rev. Lett. 33, 1404–1406 (1974).
(SLAC-SP-017 Collaboration), Phys. Rev. Lett. 33, 1406–1408 (1974).
(E288 Collaboration), Phys. Rev. Lett. 39, 252–255 (1977).
(CDF Collaboration), Phys. Rev. Lett. 74, 2626–2631 (1995).
(D0 Collaboration), Phys. Rev. Lett. 74, 2632–2637 (1995).
(Belle Collaboration, Phys. Rev. Lett. 91, 262001 (2003).
E. Eichten, K. Gottfried, T. Kinoshita, J. B. Kogut, K. D. Lane, and T. M. Yan, Phys. Rev. Lett. 34,369–372 (1975).
E. Eichten, K. Gottfried, T. Kinoshita, K. D. Lane, and T. M. Yan, Phys. Rev. D 17, 3090 (1978).
E. Eichten, K. Gottfried, T. Kinoshita, K. D. Lane, and T. M. Yan, Phys. Rev. D 21, 203 (1980).
N. Isgur and G. Karl, Phys. Lett. B 72, 109 (1977).
S. Godfrey and N. Isgur, Phys. Rev. D 32, 189–231 (1985).
S. Capstick and N. Isgur, Phys. Rev. D 34, 2809–2835 (1986).

(CMS Collaboration), Rept. Prog. Phys. 88, 087801 (2025)

(ATLAS Collaboration), arXiv:2601.11780

- 质量极大：$m = 172.56 \pm 0.31$ GeV
- 寿命极短：$\Gamma = 1.42^{+0.19}_{-0.15}$GeV
  ($\tau \sim 5 \times 10^{-25}$ S)
- 在以往的认识中，由于顶夸克的寿命极短，很难形成束缚态
- **最近，CMS和ATLAS在$t\bar{t}$阈值附近观察到了增长结构**

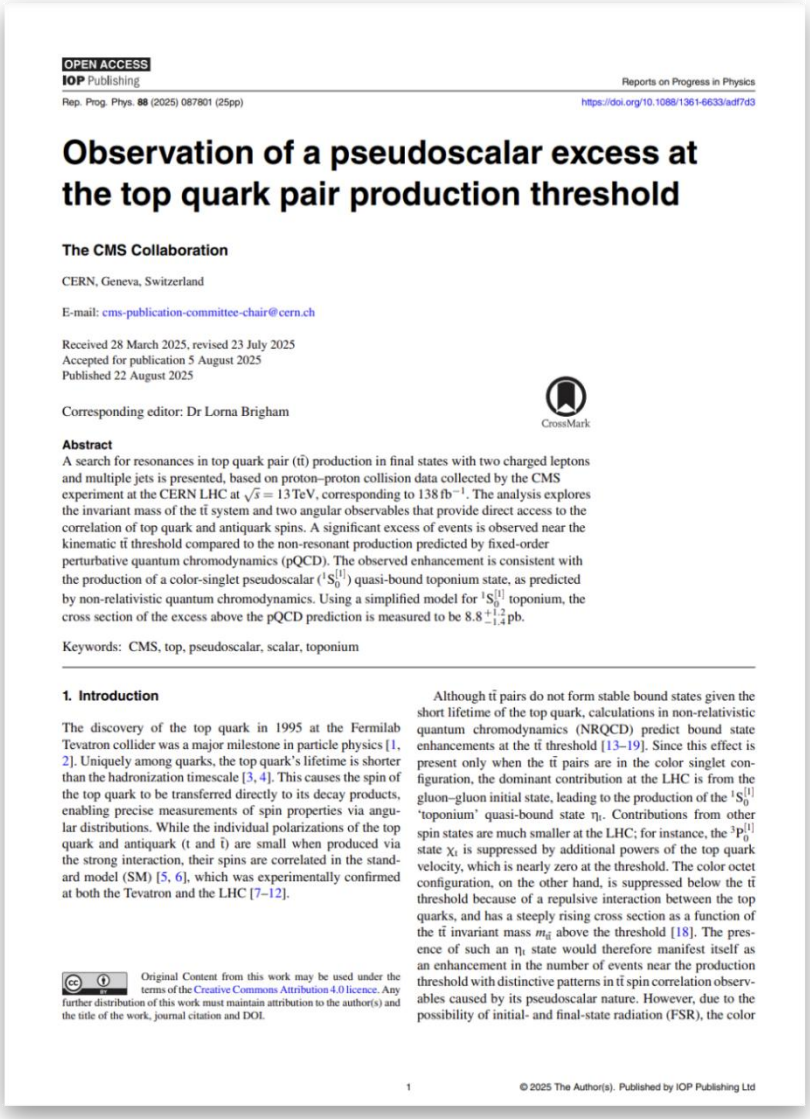

OPEN ACCESS
IOP Publishing
Reports on Progress in Physics
Rep. Prog. Phys. 88 (2025) 087801 (25pp)
https://doi.org/10.1088/1361-6633/adf7d3

Observation of a pseudoscalar excess at the top quark pair production threshold

The CMS Collaboration

CERN, Geneva, Switzerland

E-mail: cms-publication-committee-chair@cern.ch

Received 28 March 2025, revised 23 July 2025
Accepted for publication 5 August 2025
Published 22 August 2025

Corresponding editor: Dr Lorna Brigham

Abstract

A search for resonances in top quark pair ($t\bar{t}$) production in final states with two charged leptons and multiple jets is presented, based on proton–proton collision data collected by the CMS experiment at the CERN LHC at $\sqrt{s} = 13$ TeV, corresponding to 138 fb^{-1}. The analysis explores the invariant mass of the $t\bar{t}$ system and two angular observables that provide direct access to the correlation of top quark and antiquark spins. A significant excess of events is observed near the kinematic $t\bar{t}$ threshold compared to the non-resonant production predicted by fixed-order perturbative quantum chromodynamics (pQCD). The observed enhancement is consistent with the production of a color-singlet pseudoscalar ($^1S_0^{[1]}$) quasi-bound toponium state, as predicted by non-relativistic quantum chromodynamics. Using a simplified model for $^1S_0^{[1]}$ toponium, the cross section of the excess above the pQCD prediction is measured to be $8.8^{+1.2}_{-1.4}$ pb.

Keywords: CMS, top, pseudoscalar, scalar, toponium

1. Introduction

The discovery of the top quark in 1995 at the Fermilab Tevatron collider was a major milestone in particle physics [1, 2]. Uniquely among quarks, the top quark's lifetime is shorter than the hadronization timescale [3, 4]. This causes the spin of the top quark to be transferred directly to its decay products, enabling precise measurements of spin properties via angular distributions. While the individual polarizations of the top quark and antiquark (t and $\bar{t}$) are small when produced via the strong interaction, their spins are correlated in the standard model (SM) [5, 6], which was experimentally confirmed at both the Tevatron and the LHC [7–12].

Although $t\bar{t}$ pairs do not form stable bound states given the short lifetime of the top quark, calculations in non-relativistic quantum chromodynamics (NRQCD) predict bound state enhancements at the $t\bar{t}$ threshold [13–19]. Since this effect is present only when the $t\bar{t}$ pairs are in the color singlet configuration, the dominant contribution at the LHC is from the gluon–gluon initial state, leading to the production of the $^1S_0^{[1]}$ 'toponium' quasi-bound state η_t. Contributions from other spin states are much smaller at the LHC; for instance, the $^3P_0^{[1]}$ state χ_t is suppressed by additional powers of the top quark velocity, which is nearly zero at the threshold. The color octet configuration, on the other hand, is suppressed below the $t\bar{t}$ threshold because of a repulsive interaction between the top quarks, and has a steeply rising cross section as a function of the $t\bar{t}$ invariant mass $m_{t\bar{t}}$ above the threshold [18]. The presence of such an η_t state would therefore manifest itself as an enhancement in the number of events near the production threshold with distinctive patterns in $t\bar{t}$ spin correlation observables caused by its pseudoscalar nature. However, due to the possibility of initial- and final-state radiation (FSR), the color

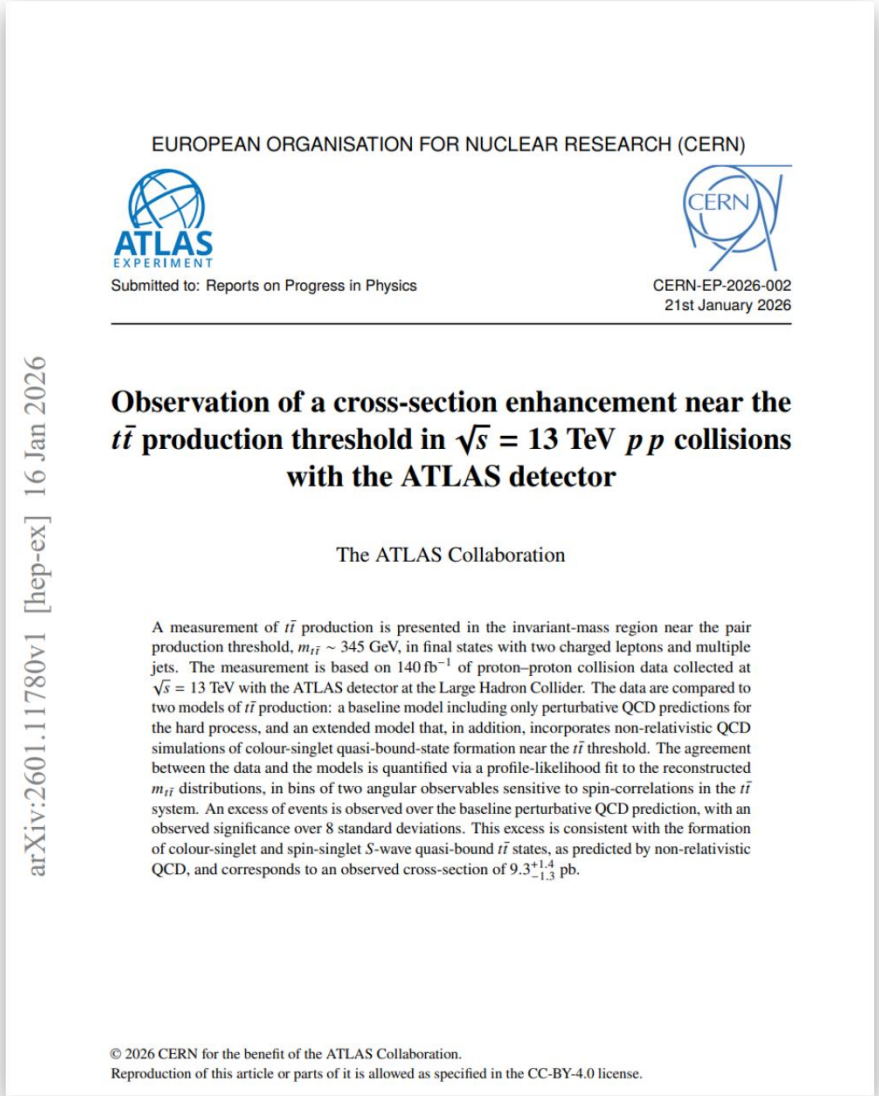

EUROPEAN ORGANISATION FOR NUCLEAR RESEARCH (CERN)

Submitted to: Reports on Progress in Physics

CERN-EP-2026-002
21st January 2026

Observation of a cross-section enhancement near the $t\bar{t}$ production threshold in $\sqrt{s}$ = 13 TeV pp collisions with the ATLAS detector

The ATLAS Collaboration

A measurement of $t\bar{t}$ production is presented in the invariant-mass region near the pair production threshold, $m_{t\bar{t}} \sim 345$ GeV, in final states with two charged leptons and multiple jets. The measurement is based on 140 fb^{-1} of proton–proton collision data collected at $\sqrt{s} = 13$ TeV with the ATLAS detector at the Large Hadron Collider. The data are compared to two models of $t\bar{t}$ production: a baseline model including only perturbative QCD predictions for the hard process, and an extended model that, in addition, incorporates non-relativistic QCD simulations of colour-singlet quasi-bound-state formation near the $t\bar{t}$ threshold. The agreement between the data and the models is quantified via a profile-likelihood fit to the reconstructed $m_{t\bar{t}}$ distributions, in bins of two angular observables sensitive to spin-correlations in the $t\bar{t}$ system. An excess of events is observed over the baseline perturbative QCD prediction, with an observed significance over 8 standard deviations. This excess is consistent with the formation of colour-singlet and spin-singlet S-wave quasi-bound $t\bar{t}$ states, as predicted by non-relativistic QCD, and corresponds to an observed cross-section of $9.3^{+1.4}_{-1.3}$ pb.

模型方法

1. Godfrey-Capstick-Isgur (GCI)模型

- 跑动耦合常数$\alpha_s(Q^2)$的参数化

$$\alpha_s(Q^2) = \sum_k \alpha_k e^{-\gamma_k Q^2}$$

- 引入抹平函数

$$\tilde{f}_{ij}(\mathbf{r}) = \int \mathrm{d}^3\mathbf{r}' \rho_{ij}(\mathbf{r}-\mathbf{r}') f(\mathbf{r}')$$

$$\sigma_{ij}^2 = \sigma_0^2 \left(\frac{1}{2} + \frac{1}{2} \left(\frac{4m_i m_j}{(m_i+m_j)^2} \right)^4 \right) + s^2 \left(\frac{2m_i m_j}{m_i+m_j} \right)^2$$

$$\rho_{ij}(\mathbf{r}-\mathbf{r}') = \frac{\sigma_{ij}^3}{\pi^{3/2}} e^{-\sigma_{ij}^2(\mathbf{r}-\mathbf{r}')^2}$$

- 引入动量依赖项

$$V_{ij}^{\mathrm{Coul}} = \beta_{ij}^{\frac{1}{2}+\epsilon_{\mathrm{Coul}}} \tilde{G}_{ij} \beta_{ij}^{\frac{1}{2}+\epsilon_{\mathrm{Coul}}} \qquad \beta_{ij} = 1 + \frac{p_{ij}^2}{(p_{ij}^2+m_i^2)^{1/2}(p_{ij}^2+m_j^2)^{1/2}}$$

$$\tilde{V}_{ij} \to \delta_{ij}^{\frac{1}{2}+\epsilon} \tilde{V}_{ij} \beta_{ij}^{\frac{1}{2}+\epsilon} \qquad \delta_{ij} = \frac{m_i m_j}{(p_{ij}^2+m_i^2)^{1/2}(p_{ij}^2+m_j^2)^{1/2}}$$

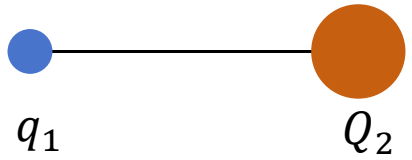

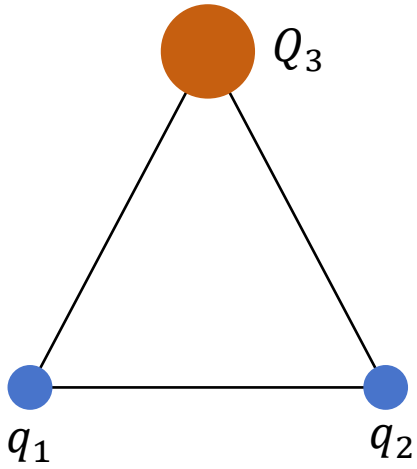

S. Godfrey and N. Isgur, Phys. Rev. D 32, 189–231 (1985).

S. Capstick and N. Isgur, Phys. Rev. D 34, 2809–2835 (1986).

- 总Hamiltonian：

$$H = \sum_i \sqrt{p_i^2 + m_i^2} + \sum_{i<j} \left(V_{ij}^{\text{Coul}} + V_{ij}^{\text{string}} + V_{ij}^{\text{cont}} + V_{ij}^{\text{so}(s)} + V_{ij}^{\text{so}(v)} + V_{ij}^{\text{tens}} \right)$$

- 单胶子交换：

$$V_{ij}^{\text{Coul}} = \beta_{ij}^{\frac{1}{2}+\epsilon_{\text{Coul}}} \tilde{G}_{ij} \beta_{ij}^{\frac{1}{2}+\epsilon_{\text{Coul}}} \qquad \tilde{G}_{ij} = C_{ij} \sum_k \frac{\alpha_k}{r_{ij}} \text{erf}(\sigma_{kij} r_{ij})$$

$$V_{ij}^{\text{cont}} = \delta_{ij}^{\frac{1}{2}+\epsilon_{\text{cont}}} \frac{2\mathbf{s}_i \cdot \mathbf{s}_j}{3m_i m_j} \nabla^2 \tilde{G}_{ij} \delta_{ij}^{\frac{1}{2}+\epsilon_{\text{cont}}}$$

$$V_{ij}^{\text{tens}} = \delta_{ij}^{\frac{1}{2}+\epsilon_{\text{tens}}} \frac{1}{3m_i m_j} \left(\frac{3(\mathbf{s}_i \cdot \mathbf{r}_{ij})(\mathbf{s}_j \cdot \mathbf{r}_{ij})}{r_{ij}^2} - \mathbf{s}_i \cdot \mathbf{s}_j \right) \times \left(\frac{1}{r_{ij}} \frac{\mathrm{d}\tilde{G}_{ij}}{\mathrm{d}r_{ij}} - \frac{\mathrm{d}^2 \tilde{G}_{ij}}{\mathrm{d}r_{ij}^2} \right) \delta_{ij}^{\frac{1}{2}+\epsilon_{\text{tens}}}$$

$$V_{ij}^{\text{so}(v)} = \frac{1}{r_{ij}} \frac{\mathrm{d}\tilde{G}_{ij}}{\mathrm{d}r_{ij}} \left(\delta_{ii}^{\frac{1}{2}+\epsilon_{\text{so}(v)}} \frac{\mathbf{r}_{ij} \times \mathbf{p}_i \cdot \mathbf{s}_i}{2m_i^2} \delta_{ii}^{\frac{1}{2}+\epsilon_{\text{so}(v)}} - \delta_{jj}^{\frac{1}{2}+\epsilon_{\text{so}(v)}} \frac{\mathbf{r}_{ij} \times \mathbf{p}_j \cdot \mathbf{s}_j}{2m_j^2} \delta_{jj}^{\frac{1}{2}+\epsilon_{\text{so}(v)}} - \delta_{ij}^{\frac{1}{2}+\epsilon_{\text{so}(v)}} \frac{\mathbf{r}_{ij} \times \mathbf{p}_j \cdot \mathbf{s}_i - \mathbf{r}_{ij} \times \mathbf{p}_i \cdot \mathbf{s}_j}{2m_i^2} \delta_{ij}^{\frac{1}{2}+\epsilon_{\text{so}(v)}} \right)$$

- 禁闭势：

$$V_{ij}^{\text{string}} = \int \mathrm{d}^3\mathbf{r}' \left(\frac{\sigma_{ij}^3}{\pi^{3/2}} \mathrm{e}^{-\sigma_{ij}^2(\mathbf{r}-\mathbf{r}')^2} \right) \left(-\frac{3}{4} C_{ij}(br_{ij} + c) \right)$$

$$= -\frac{3}{4} C_{ij} c - \frac{3}{4} C_{ij} b r_{ij} \left(\frac{\mathrm{e}^{-\sigma_{ij}^2 r_{ij}^2}}{\sqrt{\pi}\sigma_{ij} r_{ij}} + \left(1 + \frac{1}{2\sigma_{ij}^2 r_{ij}^2} \right) \text{erf}(\sigma_{ij} r_{ij}) \right)$$

$$V_{ij}^{\text{so}(s)} = \frac{1}{r_{ij}} \frac{\mathrm{d}V_{ij}^{\text{string}}}{\mathrm{d}r_{ij}} \left(-\delta_{ii}^{\frac{1}{2}+\epsilon_{\text{so}(s)}} \frac{\mathbf{r}_{ij} \times \mathbf{p}_i \cdot \mathbf{s}_i}{2m_i^2} \delta_{ii}^{\frac{1}{2}+\epsilon_{\text{so}(s)}} + \delta_{jj}^{\frac{1}{2}+\epsilon_{\text{so}(s)}} \frac{\mathbf{r}_{ij} \times \mathbf{p}_j \cdot \mathbf{s}_j}{2m_j^2} \delta_{jj}^{\frac{1}{2}+\epsilon_{\text{so}(s)}} \right)$$

S. Godfrey and N. Isgur, Phys. Rev. D 32, 189–231 (1985).

S. Capstick and N. Isgur, Phys. Rev. D 34, 2809–2835 (1986).

2. 高斯展开法(GEM)

$$\psi = \phi^{\text{color}}\phi^{\text{flavor}}\phi^{\text{spin-spatial}}$$

$$\phi^{\text{spin-spatial}} = \left[\left[s_\ell \phi^{\text{spatial}}\right]_{j_\ell} s_Q\right]_J \quad \Rightarrow \quad j-j\text{耦合}$$

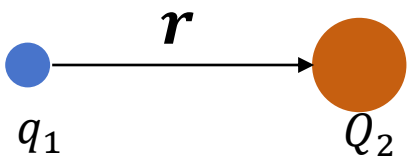

$$\phi^{\text{spatial}} = \begin{cases} \sum_n c_n \phi_{nl}(\boldsymbol{r}) & \text{介子} \\ \sum_{n_\rho n_\lambda} c_{n_\rho n_\lambda} \left[\phi_{n_\rho l_\rho}(\boldsymbol{\rho})\phi_{n_\lambda l_\lambda}(\boldsymbol{\lambda})\right]_l & \text{重子} \end{cases}$$

c_n、$c_{n_\rho n_\lambda}$通过Rayleigh-Ritz变分法求解

$$\phi_{nl}(\mathbf{r}) = N_{nl}^r e^{-\nu_n r^2} \mathcal{Y}_l(\mathbf{r}) \qquad N_{nl}^r = \left(\frac{2^{l+2}(2\nu_n)^{l+\frac{3}{2}}}{\sqrt{\pi}(2l+1)!!}\right)^{\frac{1}{2}}$$

$$\nu_n = r_{\min}^{-2}(r_{\max}/r_{\min})^{(2-2n)/n_{\max}} \qquad (n = 1 - n_{\max})$$

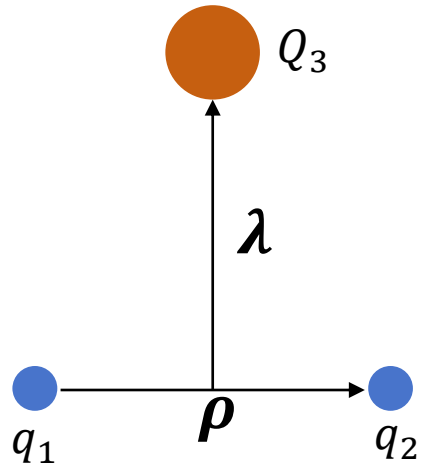

E. Hiyama, Y. Kino, and M. Kamimura, Prog. Part. Nucl. Phys. 51, 223–307 (2003).

数值结果

3.1参数拟合

本工作所用到的参数

Parameters	Meson [1]	Baryon
m_n (GeV)	0.220*	
m_s (GeV)	0.419*	
m_c (GeV)	1.428*	
m_b (GeV)	4.977*	
m_t (GeV)	172.57*	
α_k	[0.25*, 0.15*, 0.20*]	
γ_k	$\left[\frac{1}{2}^*, \sqrt{\frac{5}{2}}^*, 5\sqrt{10}^*\right]$	
b (GeV^2)	0.18*	0.141
c (GeV)	-0.253*	-0.204
σ_0 (GeV)	1.80*	1.889
s	1.55*	1.422
ϵ_{cont}	-0.168*	-0.156
ϵ_{tens}	+0.025*	-0.379
$\epsilon_{\text{so}(v)}$	-0.035*	+0.006
$\epsilon_{\text{so}(s)}$	+0.055*	+0.449
ϵ_{Coul}	0*	0*

拟合结果（重味重子）

States	Charm			Bottom		
	$M^{\text{The.}}$	$M^{\text{Exp.}}$ [2]	$M^{\text{Err.}}$ [2]	$M^{\text{The.}}$	$M^{\text{Exp.}}$ [2]	$M^{\text{Err.}}$ [2]
$\Lambda_Q(1S)$	2287.44	2286.46	0.14	5621.63	5619.60	0.17
$\Lambda_Q(2S)$	2763.16	2766.6	2.4	6042.17	6072.3	2.9
$\Lambda_Q(1P, 1/2^-)$	2606.47	2592.25	0.28	5903.02	5912.19	0.17
$\Lambda_Q(1P, 3/2^-)$	2628.01	2628.00	0.15	5911.97	5912.01	0.17
$\Lambda_Q(1D, 3/2^+)$	2878.78	2856.1	4.15	6138.52	6146.2	0.4
$\Lambda_Q(1D, 5/2^+)$	2891.72	2881.63	0.24	6145.67	6152.5	0.4
$\Sigma_Q(1S)$	2447.14	2453.97	0.14	5811.60	5810.56	0.25
$\Sigma_Q^*(1S)$	2524.30	2518.41	0.22	5839.81	5830.32	0.27
$\Xi_Q(1S)$	2475.63	2467.71	0.23	5803.15	5791.9	0.5
$\Xi_Q(2S)$	2945.59	2964.3	1.5	6221.57	...	...
$\Xi_Q(1P, 1/2^-)$	2793.46	2791.9	0.5	6084.41	6087.2	0.5
$\Xi_Q(1P, 3/2^-)$	2813.84	2816.51	0.25	6093.05	6099.8	0.6
$\Xi_Q(1D, 3/2^+)$	3062.59	3055.9	0.4	6317.44	6327.28	0.35
$\Xi_Q(1D, 5/2^+)$	3073.83	3077.2	0.4	6323.99	6332.69	0.28
$\Xi_Q'(1S)$	2581.54	2578.2	0.5	5937.06	5935.1	0.5
$\Xi_Q^*(1S)$	2651.83	2645.10	0.30	5963.15	5955.7	0.5
$\Omega_Q(1S)$	2689.86	2695.2	1.7	6037.07	6045.8	0.8
$\Omega_Q^*(1S)$	2757.73	2765.9	2.0	6062.63	...	...
$\Xi_{QQ}(1S)$	3612.30	3621.6	0.4	10174.92	...	...
$\chi^2/d.o.f. \approx 678$						

理论计算与实验测量**一致**

[1] S. Godfrey and N. Isgur, Phys. Rev. D 32, 189 (1985)

[2] Particle Data Group, Phys. Rev. D 110, 030001 (2024)

3.2顶介子与顶重子谱

顶介子谱

States	T_n	T_s	T_c	T_b
$\|1S,0^-\rangle$	0.384	0.457	-0.335	-0.702
$\|2S,0^-\rangle$	0.924	0.997	0.194	-0.161
$\|1S,1^-\rangle$	0.386	0.459	-0.332	-0.698
$\|2S,1^-\rangle$	0.925	0.998	0.195	-0.159
$\|1P,0^+\rangle_{j_\ell=\frac{1}{2}}$	0.789	0.861	0.064	-0.271
$\|1P,1^+\rangle_{j_\ell=\frac{1}{2}}$	0.790	0.862	0.065	-0.270
$\|1P,1^+\rangle_{j_\ell=\frac{3}{2}}$	0.789	0.862	0.076	-0.260
$\|1P,2^+\rangle_{j_\ell=\frac{3}{2}}$	0.790	0.862	0.077	-0.259
$\|1D,1^-\rangle_{j_\ell=\frac{3}{2}}$	1.107	1.173	0.340	-0.019
$\|1D,2^-\rangle_{j_\ell=\frac{3}{2}}$	1.108	1.173	0.341	-0.018
$\|1D,2^-\rangle_{j_\ell=\frac{5}{2}}$	1.082	1.149	0.337	-0.016
$\|1D,3^-\rangle_{j_\ell=\frac{5}{2}}$	1.083	1.149	0.338	-0.015
$\|1F,2^+\rangle_{j_\ell=\frac{5}{2}}$	1.360	1.420	0.556	0.168
$\|1F,3^+\rangle_{j_\ell=\frac{5}{2}}$	1.360	1.420	0.556	0.168
$\|1F,3^+\rangle_{j_\ell=\frac{7}{2}}$	1.326	1.387	0.546	0.168
$\|1F,4^+\rangle_{j_\ell=\frac{7}{2}}$	1.326	1.387	0.546	0.168

$$M = M_{\text{mass}} - \sum m_Q$$

(扣除重夸克质量)

顶重子谱

States	Λ_t	Ξ_t	Ξ_{nct}	Ξ_{sct}	Ξ_{nbt}	Ξ_{sbt}	Ξ_{cbt}
$\|1S,1/2^+\rangle$	0.637	0.814	0.299	0.144	0.383	0.229	-0.508
$\|1S,1/2^+\rangle$	1.016	1.193	0.658	0.464	0.741	0.555	-0.161
$\|1P,1/2^-\rangle$	0.893	1.071	0.547	0.375	0.629	0.463	-0.262
$\|1P,3/2^-\rangle$	0.894	1.071	0.547	0.375	0.629	0.463	-0.261
$\|1D,3/2^+\rangle$	1.105	1.281	0.734	0.533	0.817	0.623	-0.085
$\|1D,5/2^+\rangle$	1.105	1.281	0.734	0.533	0.818	0.623	-0.085
$\|1F,5/2^-\rangle$	1.286	1.459	0.892	0.662	0.976	0.755	0.056
$\|1F,7/2^-\rangle$	1.286	1.459	0.892	0.662	0.976	0.755	0.056

States	Σ_t	Ξ'_t	Ξ'_{nct}	Ξ'_{sct}	Ξ'_{nbt}	Ξ'_{sbt}	Ξ'_{cbt}	Ω_t	Ω_{cct}	Ω_{bbt}
$\|1S,1/2^+\rangle$	0.841	0.962	0.355	0.166	0.433	0.249	-0.487	1.057	-0.275	-0.754
$\|2S,1/2^+\rangle$	1.210	1.332	0.709	0.483	0.786	0.572	-0.144	1.423	0.078	-0.393
$\|1S,3/2^+\rangle$	0.842	0.963	0.356	0.167	0.434	0.250	-0.486	1.058	-0.274	-0.753
$\|2S,3/2^+\rangle$	1.211	1.332	0.710	0.484	0.786	0.572	-0.143	1.423	0.078	-0.393
$\|1P,1/2^-\rangle_{j_\ell=0}$	1.076	1.201	0.595	0.393	0.669	0.478	-0.248	1.293	-0.039	-0.500
$\|1P,1/2^-\rangle_{j_\ell=1}$	1.083	1.207	0.597	0.394	0.672	0.479	-0.247	1.298	-0.037	-0.498
$\|1P,3/2^-\rangle_{j_\ell=1}$	1.084	1.207	0.597	0.395	0.672	0.480	-0.246	1.298	-0.036	-0.498
$\|1P,3/2^-\rangle_{j_\ell=2}$	1.098	1.218	0.601	0.397	0.677	0.482	-0.243	1.307	-0.031	-0.495
$\|1P,5/2^-\rangle_{j_\ell=2}$	1.099	1.218	0.602	0.397	0.677	0.483	-0.243	1.308	-0.031	-0.494
$\|1D,1/2^+\rangle_{j_\ell=1}$	1.290	1.412	0.782	0.550	0.858	0.639	-0.072	1.502	0.151	-0.313
$\|1D,3/2^+\rangle_{j_\ell=1}$	1.290	1.413	0.782	0.550	0.858	0.639	-0.072	1.502	0.151	-0.313
$\|1D,3/2^+\rangle_{j_\ell=2}$	1.298	1.417	0.783	0.551	0.859	0.640	-0.071	1.506	0.153	-0.312
$\|1D,5/2^+\rangle_{j_\ell=2}$	1.298	1.417	0.783	0.551	0.860	0.640	-0.071	1.506	0.153	-0.311
$\|1D,5/2^+\rangle_{j_\ell=3}$	1.308	1.423	0.784	0.552	0.861	0.641	-0.069	1.511	0.155	-0.310
$\|1D,7/2^+\rangle_{j_\ell=3}$	1.308	1.424	0.784	0.553	0.861	0.641	-0.069	1.511	0.156	-0.309
$\|1F,3/2^-\rangle_{j_\ell=2}$	1.476	1.594	0.939	0.679	1.017	0.770	0.069	1.682	0.309	-0.167
$\|1F,5/2^-\rangle_{j_\ell=2}$	1.477	1.595	0.939	0.679	1.017	0.770	0.070	1.682	0.309	-0.167
$\|1F,5/2^-\rangle_{j_\ell=3}$	1.482	1.597	0.939	0.680	1.017	0.771	0.070	1.683	0.309	-0.166
$\|1F,7/2^-\rangle_{j_\ell=3}$	1.482	1.597	0.939	0.680	1.017	0.771	0.070	1.684	0.310	-0.166
$\|1F,7/2^-\rangle_{j_\ell=4}$	1.488	1.600	0.939	0.680	1.016	0.771	0.071	1.685	0.310	-0.165
$\|1F,9/2^-\rangle_{j_\ell=4}$	1.489	1.600	0.939	0.680	1.016	0.771	0.071	1.685	0.310	-0.165

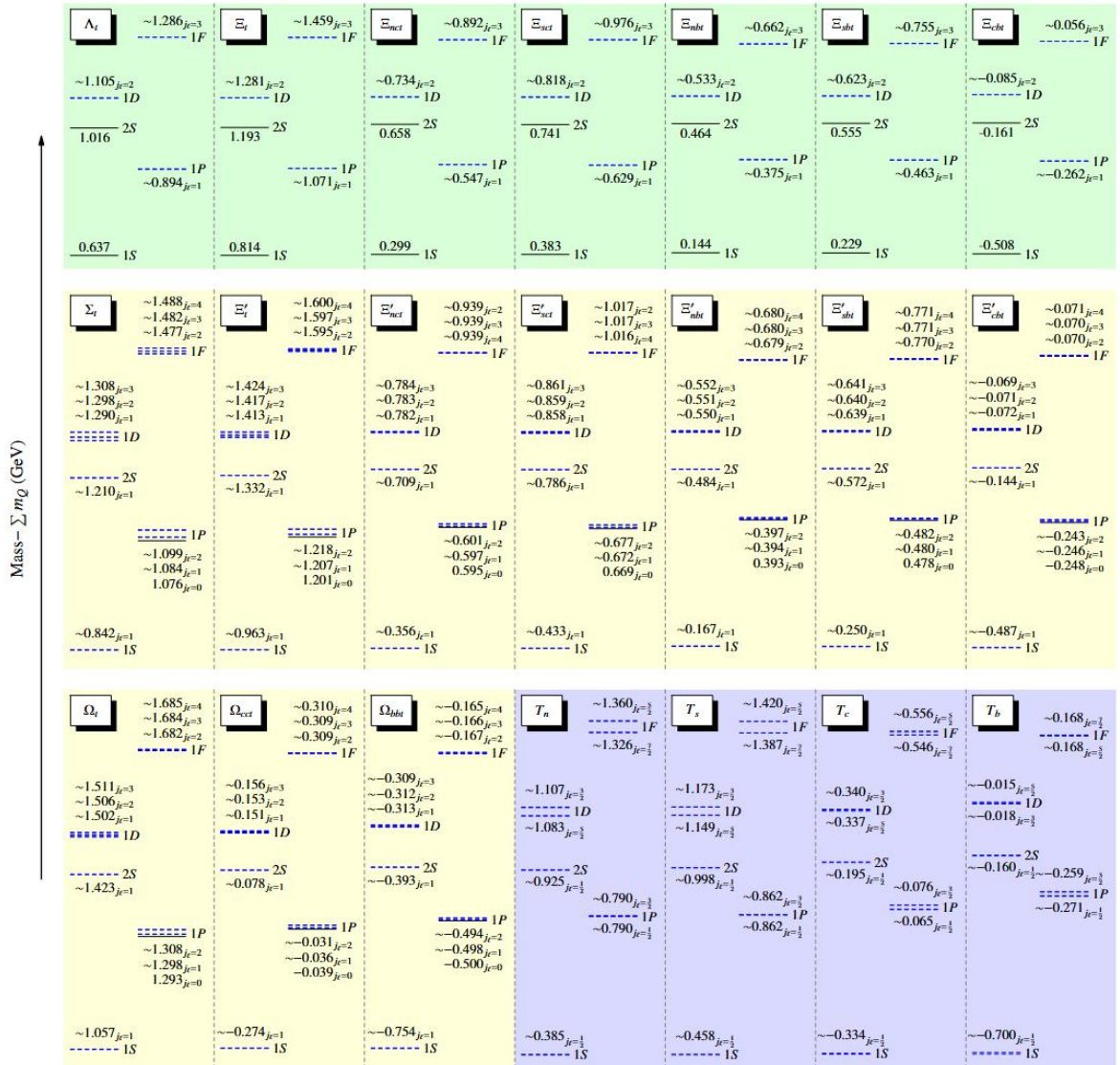

- 对称性相同的系统谱学呈现良好的对称性；
- 单顶强子中，对结果影响较大的是质量较轻的自由度；
- 较轻的自由度中，质量越大，自旋劈裂的趋势越小，“束缚”越深。

3.3 验证势模型在顶强子能区的适用性

- $V = -\frac{\kappa}{r}$

  特征值(S波)：$E_n = -\frac{1}{2}\mu\kappa^2$

- $V = br$

  特征值(S波)：$E_n = -\left(\frac{b^2}{2\mu}\right)^{\frac{1}{3}} z_n$

  z_n为Airy函数Ai(z)的零点

  $z_1 \approx -2.33811, z_2 \approx -4.08795, z_3 \approx -5.52056 \cdots$

- $V = -\frac{\kappa}{r} + br + c$

  没有简洁且通用的**解析解**

  通常采用**近似解**或**数值解**

基态解随约化质量μ的变化关系

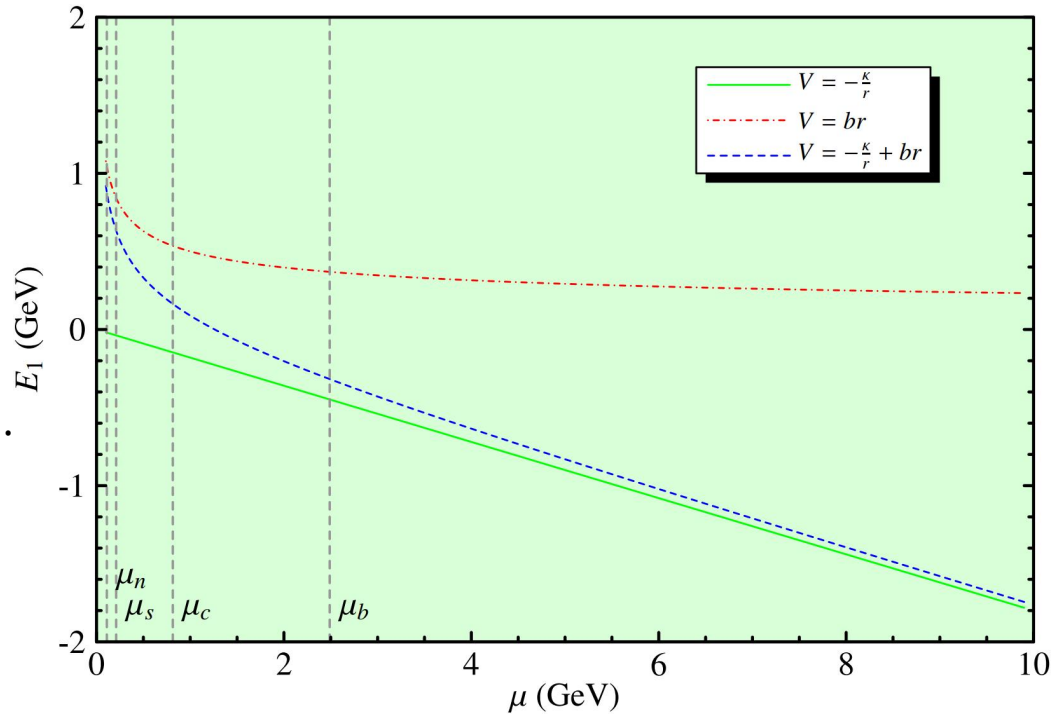

参数：

$\kappa = 0.6$

$b = 0.14\ \mathrm{GeV}^2$

$c = 0$

覆盖了$m_n \sim m_b$ ($\mu = \frac{m_q}{2}$)

继续增大约化质量μ的结果

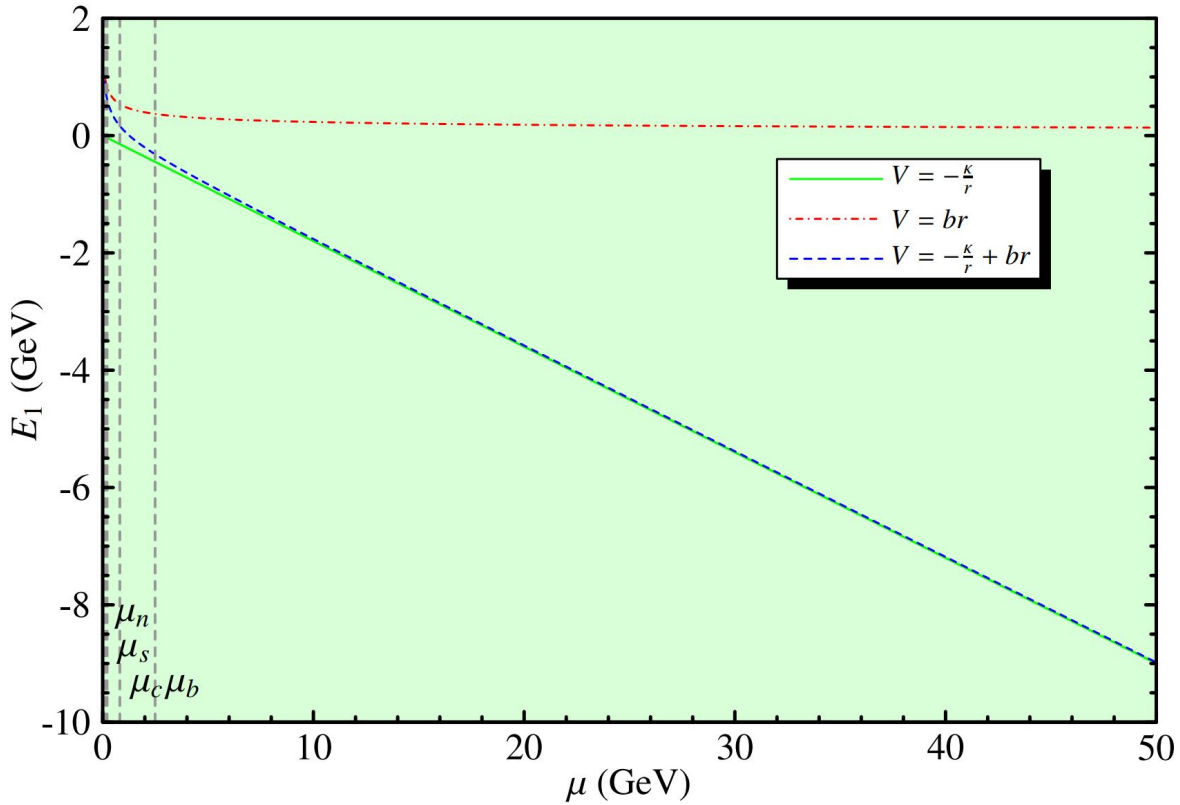

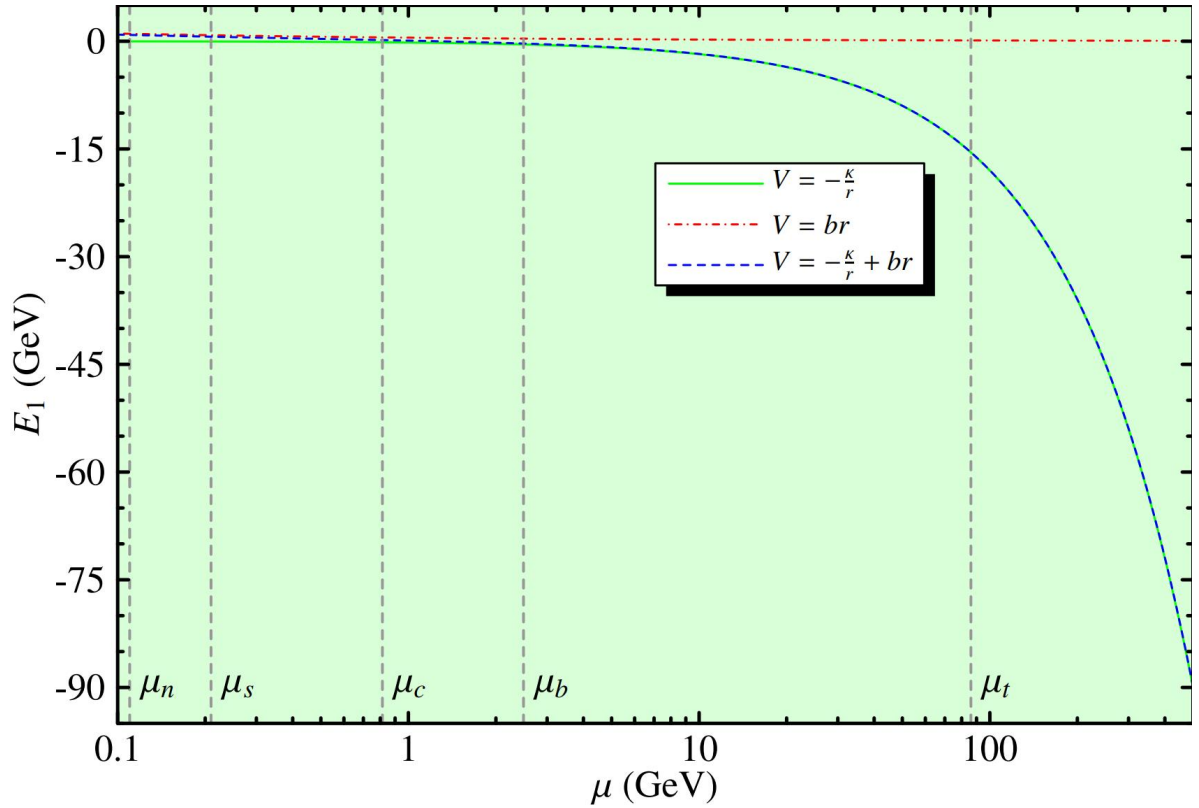

$V = -\frac{\kappa}{r} + br + c$的结果：

- 增大约化质量，E_1的变化非常明显
- 约化质量很大时，$E_1 \sim -\frac{1}{2}\mu\kappa^2$（与纯库仑势的结果接近）
- $\mu = \mu_t$时，$E_1 \approx -15.46$ GeV

GCI模型中的类库仑势

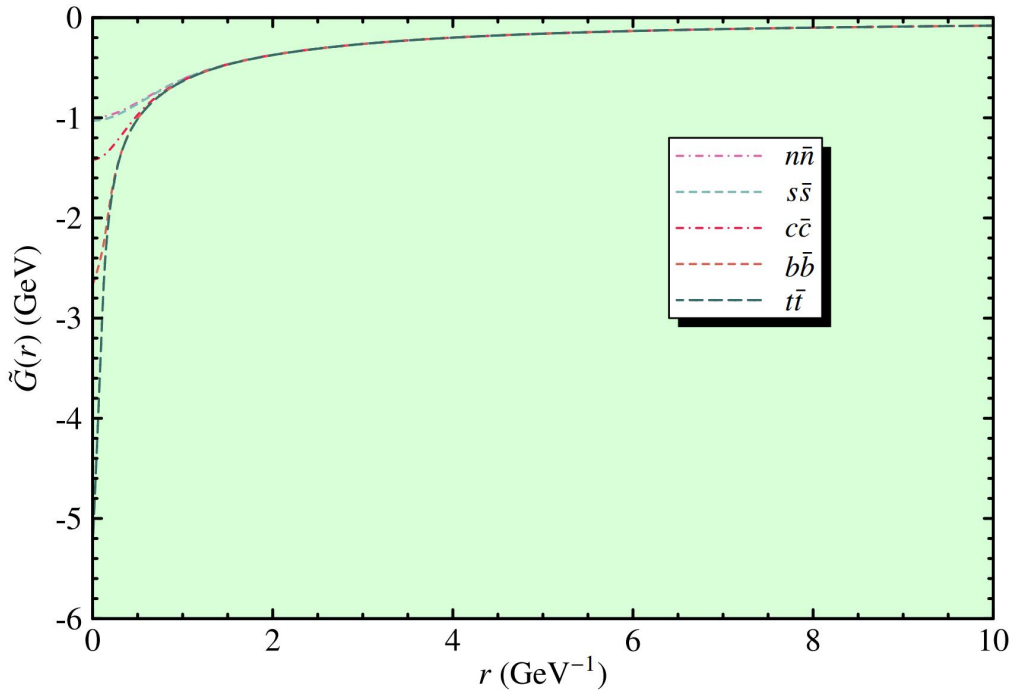

精确测量$t\bar{t}$的质量是验证势模型在大m_Q能否适用的关键，为研究单胶子交换势及禁闭势（常数项）提供重要信息

(CMS Collaboration), Rept. Prog. Phys. 88, 087801 (2025)

The η_t mass and width are set to 343 and 2.8 GeV, respectively, corresponding to the expectation that the toponium mass is twice m_t minus a binding energy of about 2 GeV [17], and its decay width is twice the width of the top quark [13]. The

[13] Fadin V S, Khoze V A, and Sjöstrand T, Z. Phys. C 48, 613 (1990)
[17] Fuks B, Hagiwara K, Ma K, and Zheng Y-J, Phys. Rev. D 104, 034023 (2021)

GCI模型随夸克质量增大时的解

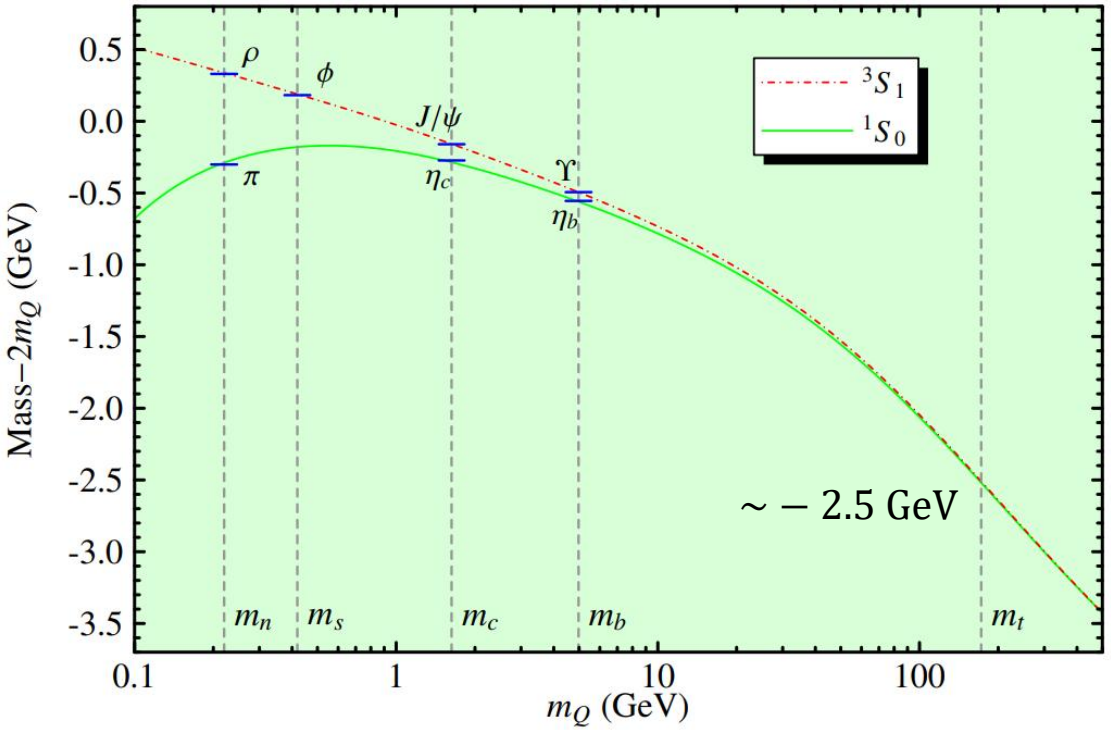

- 随着m_Q的增大，自旋单态和三重态的质量差逐渐缩小
- 该结果在$m_n(\pi-\rho)$、$m_s(\phi)$、$m_c(\eta_c-J/\psi)$、$m_b(\eta_b-\Upsilon)$中符合地较好
- $m_Q=m_t$时，Mass $-2m_Q \approx -2.5$ GeV
- 随着m_Q的增大，GCI与Cornell势的结果趋势不同

(ATLAS Collaboration), arXiv:2601.11780

sample was produced in MadGraph 3.5.5 with the NNPDF3.0nlo PDF set. The η_t mass is set to 343 GeV, in line with the expectation that the mass of the $t\bar{t}$ quasi-bound ground state is twice that of the top quark minus a binding energy of about 2 GeV [18, 31]. Its total width is set to 2.8 GeV, i.e. roughly twice that

[18] Y. Sumino and H. Yokoya, JHEP 09, 034 (2010)
[31] B. Fuks, K. Hagiwara, K. Ma and Y.-J. Zheng, Phys. Rev. D 104, 034023 (2021)

3.4 单顶强子—接近理想的重夸克系统

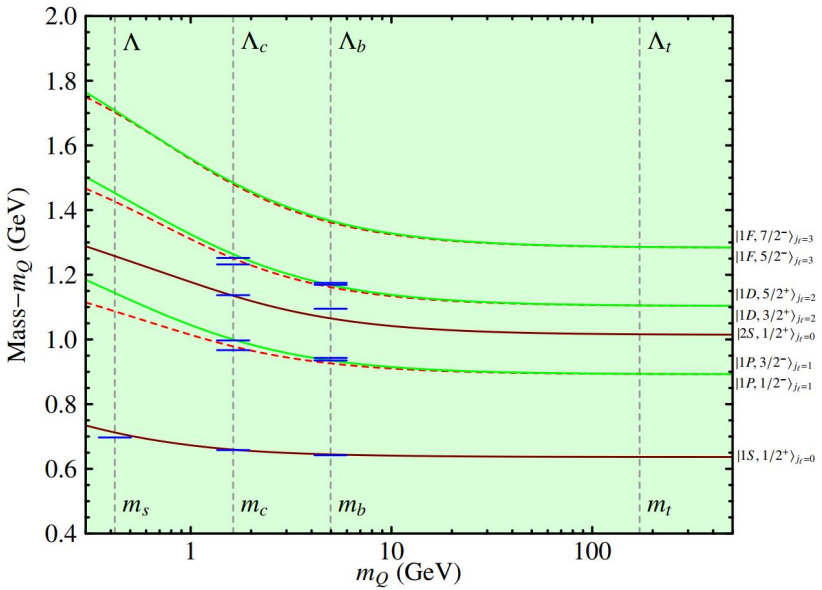

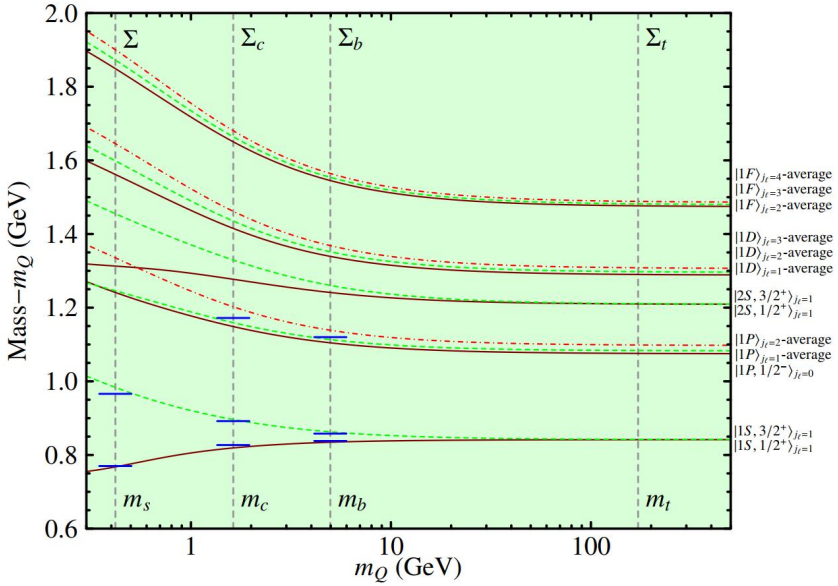

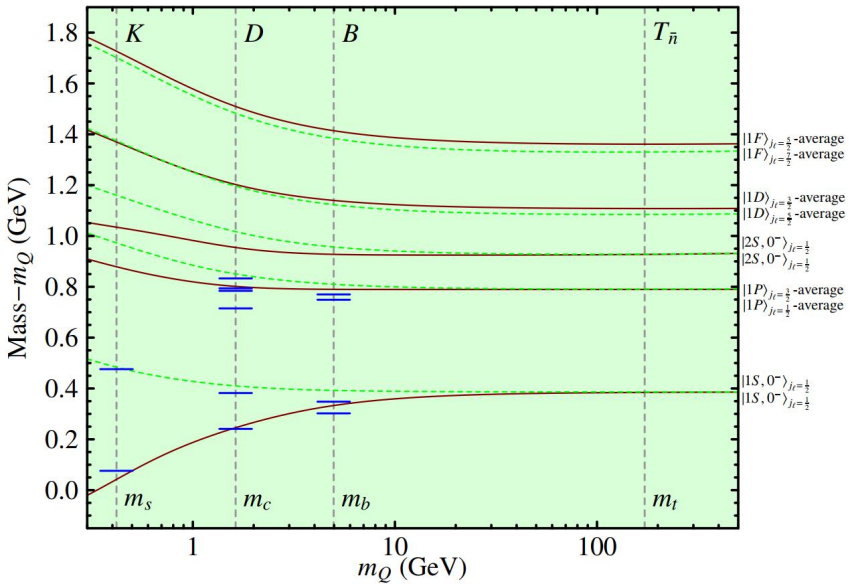

$m_Q \to \infty$时，包含m_Q的项：

- 势模型参数→不变
- $\sqrt{p^2 - m_Q^2} - m_Q \to 0$
- $\frac{1}{m_q m_Q} \to 0$，$\frac{1}{m_Q^2} \to 0$
- $\beta_{ij} \sim 1$，$\delta_{ij} \sim 1$

- 同一个$|NL, J^P\rangle_{j_\ell}$中，$J = j_\ell + \frac{1}{2}$和$J = |j_\ell - \frac{1}{2}|$的结果随$m_Q$的增大趋近于一个常数；
- $|NL\rangle$相同，j_ℓ不同时，结果随m_Q的增大可能趋近于不同的常数；
- 单顶强子系统可以很好地反映重夸克对称性。

总结

1. 实验上发现了大量的轻强子、重味介子、重味重子；势模型可以较好地处理从轻强子到粲强子，再到底强子的谱学问题；本工作使用GCI模型计算了单顶介子和重子谱。

2. 理论上可以很可地描述从π到$b\bar{b}$的夸克偶素谱学，测量$t\bar{t}$的质量可以检验势模型在大的夸克质量下的适用性。

3. 单顶强子接近理想的重夸克系统，其表现出的重夸克对称性明显优于单粲和单底强子。

谢谢各位批评指正